A Simple and Widely Applicable Method to ^{59}Fe-Radiolabel Monodisperse Superparamagnetic Iron Oxide Nanoparticles for *In Vivo* Quantification Studies

Barbara Freund,[†,*] Ulrich I. Tromsdorf,[∥] Oliver T. Bruns,[#] Markus Heine,[‡] Artur Giemsa,[†] Alexander Bartelt,[†,§] Sunhild C. Salmen,[∥] Nina Raabe,[⊥] Joerg Heeren,[†] Harald Ittrich,[⊥] Rudolph Reimer,[¶] Heinrich Hohenberg,[¶] Udo Schumacher,[‡] Horst Weller,[∥] and Peter Nielsen[†,*]

[†]Department of Biochemistry and Molecular Cell Biology, [‡]Department of Anatomy and Experimental Morphology, [§]Department of Orthopaedics, and [⊥]Department and Clinic of Diagnostic and Interventional Radiology, University Medical Center Hamburg-Eppendorf, D-20246 Hamburg,Germany, [∥]Institute of Physical Chemistry, Universität Hamburg, 20146 Hamburg, Germany, [¶]Department of Electron Microscopy and Micro Technology, Heinrich-Pette Institute, 20251 Hamburg, Germany, and [#]Department of Chemistry, Massachusetts Institute of Technology, Cambridge, Massachusetts 02139, United States

ABSTRACT A simple, fast, efficient, and widely applicable method to radiolabel the cores of monodisperse superparamagnetic iron oxide nanoparticles (SPIOs) with ^{59}Fe was developed. These cores can be used as precursors for a variety of functionalized nanodevices. A quality control using filtration techniques, size-exclusion chromatography, chemical degradation methods, transmission electron microscopy, and magnetic resonance imaging showed that the nanoparticles were stably labeled with ^{59}Fe. Furthermore, the particle structure and the magnetic properties of the SPIOs were unchanged. In a second approach, monodisperse SPIOs stabilized with ^{14}C-oleic acid were synthesized, and the stability of this shell labeling was studied. In proof of principle experiments, the ^{59}Fe-SPIOs coated with different shells to make them water-soluble were used to evaluate and compare *in vivo* pharmacokinetic parameters such as blood half-life. It could also be shown that our radiolabeled SPIOs embedded in recombinant lipoproteins can be used to quantify physiological processes in closer detail than hitherto possible. *In vitro* and *in vivo* experiments showed that the ^{59}Fe label is stable enough to be applied *in vivo*, whereas the ^{14}C label is rapidly removed from the iron core and is not adequate for *in vivo* studies. To obtain meaningful results in *in vivo* experiments, only ^{59}Fe-labeled SPIOs should be used.

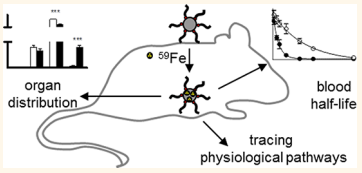

KEYWORDS: SPIOs · ^{59}Fe labeling · *in vivo* quantification · ^{14}C-oleic acid · blood half-life

Superparamagnetic iron oxide nanoparticles (SPIOs) have been used as contrast agents in magnetic resonance imaging (MRI) over the last two decades. Due to their valuable magnetic properties and their rather low toxicity, they have a considerable potential in nanomedicine and in fundamental biological research.[1−4] First generation contrast agents such as Endorem or Resovist consisted of polydisperse iron oxide cores coated with dextran or carboxydextran and were used mainly for the detection and characterization of small focal liver lesions.[5−7] They are produced in aqueous solution at low temperature by co-precipitation of ferrous and ferric iron salts in the presence of the respective carbohydrates as stabilizers. Originating from their syntheses, these SPIOs have, however, limitations as they are polydisperse, of poor crystallinity, and have therefore inferior magnetic properties.[8] In order to improve these characteristics, different synthetic strategies to produce monodisperse and highly crystalline SPIOs have been developed. They are mainly based on the decomposition of organometallic precursors in high boiling solvents.[9,10]

For a transfer from laboratory to biological and clinical application, detailed information on pharmacokinetic parameters of an individual nanodevice is mandatory. Among these are the blood half-life, the detailed *in vivo* distribution, the degradation and/or storage of nanoparticles, as well as their acute and chronic toxicity.[11,12] A reliable quantification system is also desirable for many other biological applications of SPIOs such as tumor targeting, drug delivery, or transfer of SPIOs through biological barriers. *In vivo* quantification cannot be derived from MRI studies alone, as the correlation of relaxivities to local particle concentration is difficult to determine due to possible agglomeration and increase of

* Address correspondence to nielsen@uke.de, b.freund@uke.de.

Received for review June 1, 2012 and accepted July 14, 2012.

Published online July 14, 2012
10.1021/nn3024267

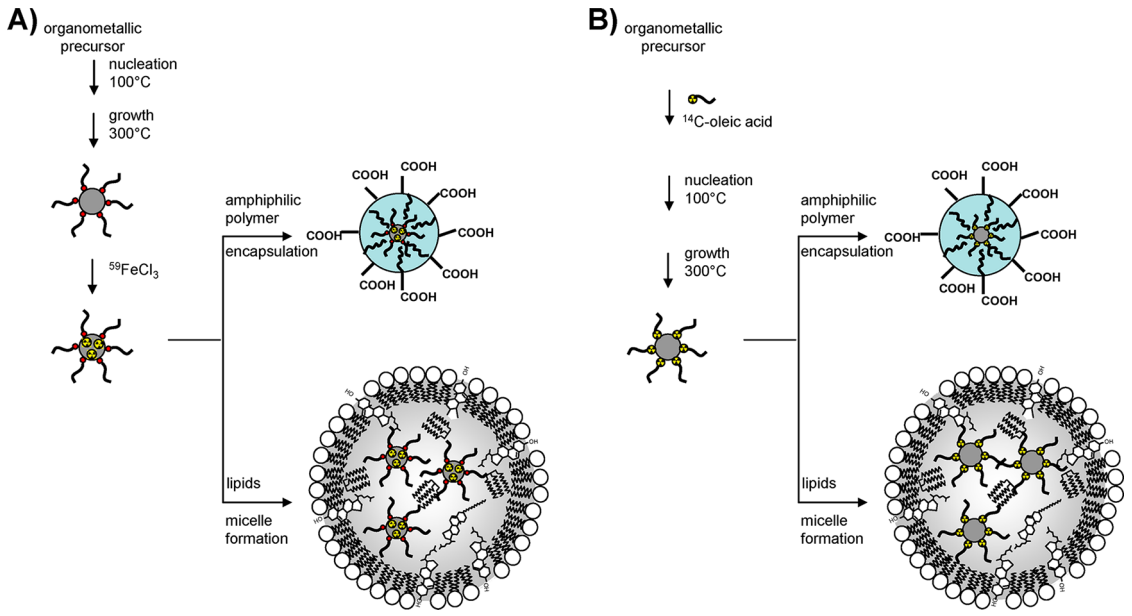

Figure 1. Possible core (^{59}Fe) and shell (^{14}C) labeling of SPIOs. (A) Hydrophobic SPIOs covered by oleic acid are incubated with a tracer dose of ^{59}Fe. (B) [1-^{14}C]-oleic acid is used as stabilizer in the synthesis of SPIOs. The radiolabeled hydrophobic cores can be transferred into the aqueous phase by encapsulation with an amphiphilic polymer or be embedded directly into recombinant lipoproteins (nanosomes). From the results of the ^{14}C experiments (see text), we conclude that the polymer-coated SPIOs contain low amounts of oleic acid which is replaced by the polymer during encapsulation.

hydrodynamic diameters caused by opsonization.[2,8] In addition, most tissues contain substantial background iron concentrations which can even be higher than the amount of iron contributed from the injected SPIOs, which makes it very difficult to rely on iron quantification techniques such as atom absorption spectroscopy.

To follow the particle *in vitro* and *in vivo*, the shells of different types of nanoparticles, including SPIOs, have been modified by fluorescent[13,14] or radioactive labels.[15,16] Fluorescent tags are very attractive for cell biological studies, but *in vivo* quantification of fluorescent nanoparticles is hard to achieve. Additionally, SPIOs often quench the attached fluorophores. Nanoparticles with a radionuclide attached to the surface by a spacer group have been used mainly for PET or SPECT studies.[17,18] However, the stability of these nanoconstructs *in vivo* is an open question, and a separation of the label from the nanoparticle core can occur in the body which would influence all quantitative measurements of the particles.

Labeling of the nanoparticle core before or after synthesis should therefore be more reliable for most *in vivo* quantification studies.[19] For dextran- or carboxydextran-coated SPIOs used as MRI contrast agents (Endorem, Resovist), a core labeling with ^{59}Fe by chemical synthesis has been used in studies involved in the registration procedure.[5,20−23] While it is possible to adapt this method for a given co-precipitation synthesis, it is hardly transferable to a high-temperature synthesis of modern monodisperse SPIOs. One reason is that the frequently used iron precursor $Fe(CO)_5$ is not commercially available in radiolabeled form and cannot be prepared on a small scale in a standard laboratory. In addition, a miniaturization of a particle synthesis with identical high quality of nanoparticles is hard to achieve. However, this is absolutely required in order to obtain a reasonable high specific radioactivity which allows a sensitive quantification of smaller fractions of the injected dose in a given organ. A low specific radioactivity would make it necessary to inject higher amounts of SPIOs, a fact that could influence the transport and uptake of SPIOs.[23]

A postsynthetic technique, such as neutron activation has been successfully applied for Au nanoparticles.[24−27] However, for natural iron (^{58}Fe (n, γ) ^{59}Fe) with its low content of ^{58}Fe (0.28%), rather long radiation times are required which inevitably give rise to heat damage to organic materials, such as oleic acid, which stabilize SPIOs by preventing agglomeration. An alternative using proton activation of ^{56}Fe in SPIOs (^{56}Fe (p, n) ^{56}Co) was recently described which yields a ^{56}Co-labeled iron core.[28] So far, this approach was tested in cell models but can hardly be used to follow the degradation of SPIOs *in vivo* because the Co label would follow different transport ways compared to iron.

In the present work, we describe a widely usable postsynthetic method to ^{59}Fe-radiolabel iron oxide cores of monodisperse SPIOs derived by a high-temperature synthesis. It allows the SPIOs to be fully characterized before labeling and bears a low radiation burden for the experimenter. It takes place at room temperature, and even small amounts can be labeled quasi "on-demand". After demonstrating the stability of the ^{59}Fe labeling in different approaches *in vitro*, we

compared, in a proof of principle *in vivo* application, the blood half-lives of differently coated SPIOs in mice. Using ^{59}Fe-SPIOs embedded in recombinant lipoproteins so-called "nanosomes", we also demonstrated that this label can be used to follow and quantify physiological lipoprotein transport pathways in detail.[29,30]

Our work offers the possibility to use these radiolabeled cores for the preparation of a variety of modern functionalized iron-oxide-based nanodevices.

RESULTS AND DISCUSSION

Synthesis and Quality Control. For core labeling with ^{59}Fe, oleic-acid-stabilized monodisperse SPIOs in chloroform were incubated with a water-free tracer dose of $^{59}FeCl_3$, a hard γ-emitter (1.1, 1.3 MeV) (Figure 1A). The second labeling strategy used [1-^{14}C]-oleic acid as ligand in the high-temperature synthesis (Figure 1B), which forms a stabilizing ligand shell.

For the incubation with ^{59}Fe, iron oxide cores with different diameters (4, 6, 10, or 12 nm) were used,[26,27] all stabilized with oleic acid and dissolved in an organic solvent such as chloroform. The amount of ^{59}Fe atoms equaled 0.01−0.5% of the iron in the SPIOs. After 24 h, about 60% of the label was found in the organic phase in contrast to free Fe ions that would be located in the aqueous phase (see Supporting Information). Repeated extraction of the chloroform phase with water or 1 mM ethylenediaminetetraacetic acid (EDTA) solution, a strong chelator for ionic Fe^{3+}, removed only a small amount of the ^{59}Fe activity (3−5%). This suggests that the ^{59}Fe ions were incorporated into the core and not merely dissolved in the organic phase. This is supported by the fact that, after precipitation with acetone, 96% of the radioactivity was found in the pellet (data not shown). This incorporation is probably based on the circumstance that the oleic acid on the particle surface is in equilibrium with the free oleic acid in the solvent and can form iron oleate with the added ^{59}Fe. Iron oleate is the precursor for crystal growth in most high-temperature syntheses,[31−33] and it is likely that to a small extent this reaction may also take place at room temperature, being enough for the tracer dose to be incorporated. This process seems to be very fast: it cannot be accelerated by the addition of oleic acid and takes place in different organic solvents (hexane, chloroform, and toluene). The size of the particle seems to have a minor effect on the incorporation, while the addition of EDTA or vitamin C, a reducing agent, almost completely suppresses the incorporation (see Supporting Information). The incorporation process can be saturated: when increasing the dose of added free iron up to a 10 000-fold, the incorporation was significantly reduced and more unbound ^{59}Fe was found in the supernatant after precipitation with acetone (see Supporting Information). Macroscopically, a brown solid formed, supposedly iron oxide. It should be noted that the ion exchange reaction described here is in accordance with earlier experiments. Egger stirred a ^{59}Fe-labeled Fe_3O_4 bulk material in a ferrous chloride solution and followed the isotopic exchange. The reaction consisted of an initially fast surface reaction followed by a slower diffusion-controlled reaction.[34] Similar reactions are known for quantum dots. The cations of a quantum dot crystal lattice can be replaced completely by stirring in a solution containing an excess of a different cation.[35,36]

For *in vivo* studies and further quality controls, the SPIOs were transferred into aqueous medium by encapsulation with a well-characterized amphiphilic polymer: poly(maleic anhydride-*alt*-1-octadecene).[37,38]

When the now water-soluble SPIOs were dialyzed against a buffer, less than 3% of the ^{59}Fe activity could be found in the dialysate after 24 h. This appears to be free ^{59}Fe from the encapsulation procedure, as after 24 and 48 h with buffer changes the amount of activity was well below 1% (data not shown). As this small amount of free ^{59}Fe could also be removed by a centrifugal filtering device (5 kDa) (see Supporting Information), a filtration step was performed before all experiments. The size-exclusion chromatography (SEC) of polymer-coated ^{59}Fe-labeled SPIO showed a peak at 15 min representing the small fraction of aggregated SPIOs and a broad peak at 25 min when the monodisperse coated SPIOs are eluted. ^{59}Fe activity and iron were strictly coeluted in all fractions (Figure 2A). The elution profile completely resembles the one of the unlabeled polymer-coated SPIOs. When incubating already polymer-coated SPIOs with a tracer dose of ^{59}Fe, only free ^{59}Fe could be detected in the SEC (Figure 2B), showing that the elution profile is not an artifact of the interaction between the negatively charged shell and the Fe cation.

In order to check if the label was also stable in biological media, we incubated polymer-coated SPIOs in fetal calf serum (FCS) and performed a size-exclusion chromatography. The opsonization with plasma proteins increased the size of the particles, but no free ^{59}Fe could be detected (see Supporting Information). Furthermore, we used centrifugal filter devices (5 kDa), and the polymer-coated SPIOs were incubated in PBS or FCS. After the first centrifugation, about 1% of the radioactivity could be found in the filtrate corresponding to the earlier described free ^{59}Fe. Resuspension and further centrifugation showed no activity in the filtrate of the PBS or FCS probe (see Supporting Information), suggesting that our label is stable in PBS and biological media.

To make sure that the SPIOs were not altered in size distribution, morphology, and aggregation behavior, standard and labeled batches were compared in the transmission electron microscope (TEM) and in MRI phantoms. As shown in Figure 2C−E, no differences between unlabeled and labeled SPIOs could be detected, indicating that postsynthetic ^{59}Fe radiolabeling did not change the properties of SPIOs.

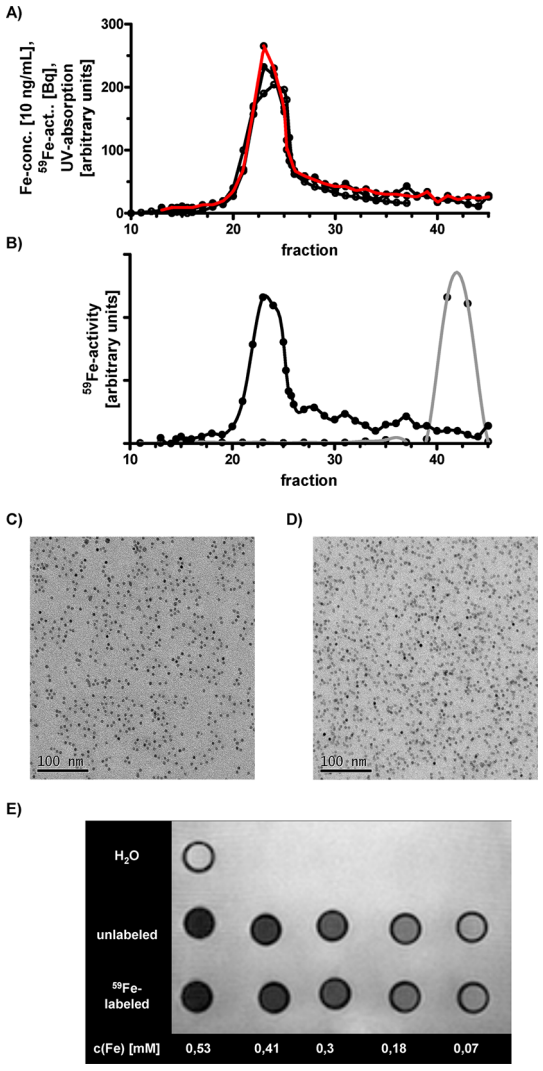

Figure 2. Quality control of ^{59}Fe-labeled monodisperse SPIOs. (A) Size-exclusion chromatography (SEC) of ^{59}Fe-labeled SPIOs (10 nm iron core, amphiphilic polymer) on a Superose 6 column. UV absorption (white circles), ^{59}Fe activity (black circles), and iron (red circles) were measured in fractions. (B) SEC of hydrophilic SPIOs that were incubated with ^{59}Fe before (black circles) or after (gray circles) encapsulation with an amphiphilic polymer (10 nm core size). TEM images of unlabeled (C) and ^{59}Fe-labeled (D) polymer-coated SPIOs (6 nm core) cast from aqueous solution (for higher magnification image, see Supporting Information). (E) Comparison of the T_2* contrast of standard and ^{59}Fe-labeled SPIOs in MRI.

To further investigate the label, SPIOs were slowly dissolved in acid solution and the release of iron and ^{59}Fe activity was monitored. Using two different acid concentrations, the release of stable and radioactive iron isotopes followed similar kinetics (see Supporting Information). This demonstrates that the ^{59}Fe label is representative for the core iron.

In a second approach, [1-^{14}C]-oleic acid was used in the particle synthesis to label the shell of SPIOs. After precipitating and resuspending the hydrophobic SPIOs with ethanol, the amount of ^{14}C-oleic acid in the supernatant decreased and most of the unbound oleic acid was removed after a third wash (Figure 3A). When [1-^{14}C]-oleic acid-labeled SPIOs (^{14}C-SPIOs) were then stirred with different amounts of nonlabeled oleic acid, most of the radiolabel was replaced by the added nonradioactive oleic acid (Figure 3B). These results show that oleic acid is not statically bound to the particles, but is in equilibrium with free oleic acid in the solvent.

The same effect was seen when the ^{14}C-SPIOs were incubated with different amounts of the amphiphilic polymer. Even at low concentrations, close to all of the ^{14}C-oleic acid is replaced by the polymer (Figure 3C). This result is in contrast to the results of Shtykova *et al.* that showed that hydrophobic alkane chains of the amphiphilic polymer interact with the tails of oleic acid on the surface of SPIOs while the hydrophilic acid function renders SPIOs water-soluble.[37] Our findings suggest that the oleic acid is replaced by the polymer. However, under the conditions used (undried solvents, no inert gas conditions), we cannot fully exclude that hydrolysis of the anhydride function of the polymer took place. Also, the precipitation by addition of ethanol may have altered the binding of the polymer, here; further investigations would be needed. Still our results show that the oleic acid labeling cannot be used to generate radiolabeled polymer-coated SPIOs.

The easy exchange of oleic acid from the iron oxide cores was also shown *in vivo* when the biodistribution of lipophilic ^{14}C-SPIOs was studied in mice. We used nanosomes, triglyceride-rich micelles in which various lipophilic nanoparticles can be embedded. It was shown earlier that these micelles form *in vivo* "chylomicron-like" lipoproteins and are processed as natural lipoproteins in the circulation.[29,39] In our approach, these nanosomes were labeled with the ^{14}C-SPIOs and injected into the tail vein of mice. After sacrificing, radioactivity in the organs was measured and compared to the organ distribution of mice injected with nanosomes double-labeled with ^{59}Fe-SPIOs and ^{3}H-triolein, a triglyceride that naturally occurs in chylomicrons (Figure 4). It showed that both radioisotopes of the double-labeled nanosomes showed a similar organ distribution. In contrast, injection of nanosomes labeled with ^{14}C-SPIOs resulted in a completely different organ uptake (Figure 4), suggesting that most of the labeled oleic acid shell is separated from the iron oxide cores already in the bloodstream and excreted *via* the kidneys. These results suggest that the [1-^{14}C]-oleic-acid-coated SPIOs cannot be used to follow the fate of SPIOs *in vivo*, whereas the ^{59}Fe label is well-suited for these kinds of studies.

Measuring Pharmacokinetic Parameters. Radiolabeled nanoparticles can be used to determine their pharmacokinetic behavior, a prerequisite of a compound investigated for application in humans. We used ^{59}Fe-SPIOs to determine the blood half-life of nanosomes and compared it to the one of polymer-coated SPIOs.

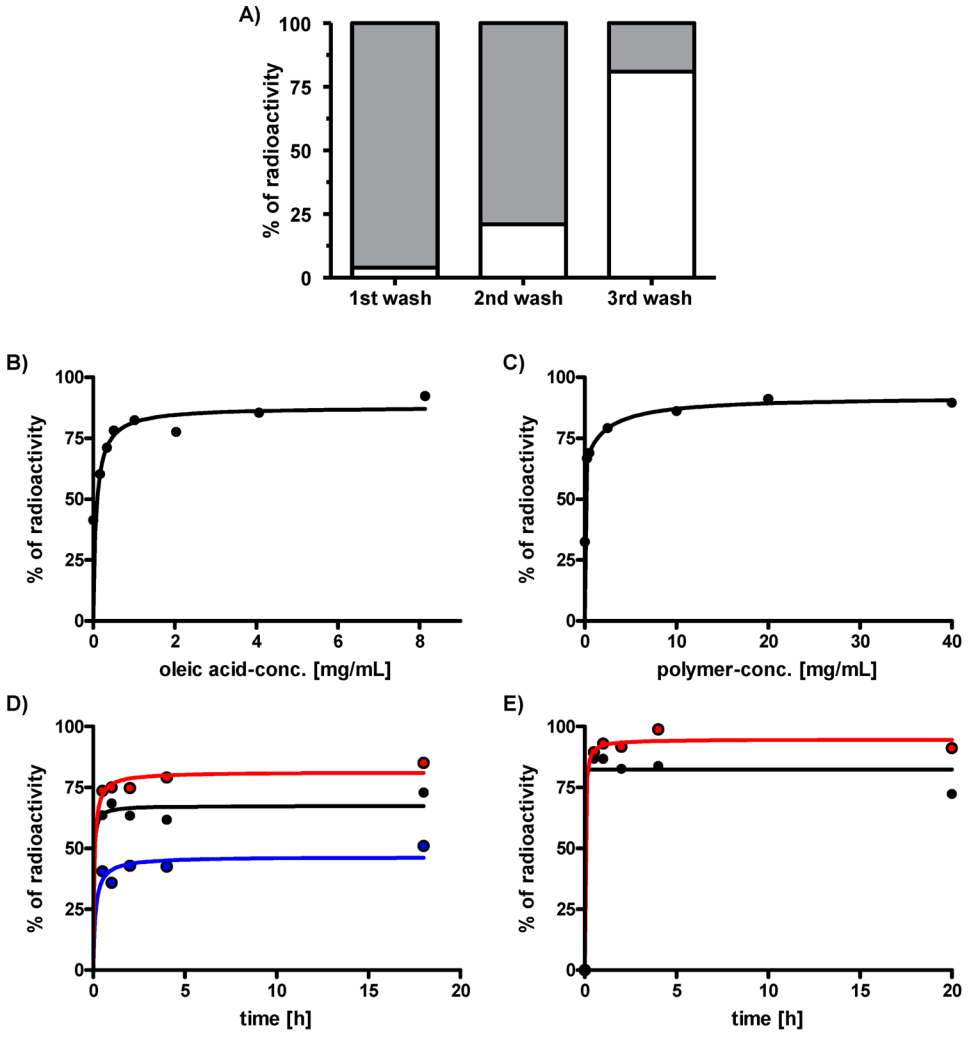

Figure 3. Replacement of [1-^{14}C]-oleic acid from SPIOs. (A) Distribution of ^{14}C radioactivity between pellet (white bar) and supernatant (gray bar) after precipitation. (B) Incubation of SPIOs with different concentrations of oleic acid or amphiphilic polymer (C). (D) Replacement of ^{14}C-oleic acid when stirred with no (blue), 0.5 mg/mL (black), and 8.1 mg/mL (red) oleic acid in the solution. (E) Replacement of ^{14}C-oleic acid when stirred with 0.5 mg/mL (black) and 20 mg/mL (red) of polymer in the solution.

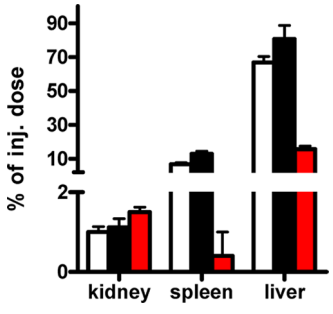

Figure 4. Organ distribution of the radioactive labels 15 min after i.v. injection. Nanosomes were labeled with ^{3}H-triolein (white bars) and ^{59}Fe-SPIOs (black bars), or SPIOs coated with [1-^{14}C]-oleic acid (red bars) and i.v. injected into FVB mice. Mean values in % of added radioactivity ± sem with $n \geq 6$.

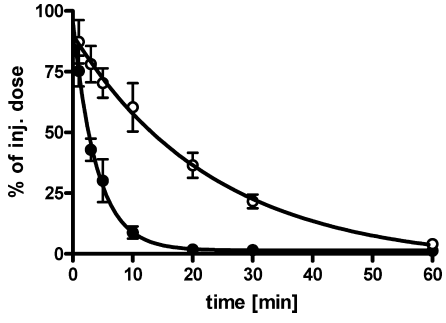

Figure 5. Impact of the coating on the blood half-life of radioactive-labeled SPIOs. Nanosomes (black dots) or polymer-coated SPIOs (white dots) were injected into the tail veins of BALB/C mice. Mean values ± sem with $n \geq 4$. Curves represent an exponential fit using a one-compartment model.

As expected from their large size (200 nm), half of the recombinant lipoproteins were cleared from the bloodstream after 3 min while the polymer-coated SPIOs showed a longer blood half-life of 16 min (Figure 5). The amount of radioactivity and iron used in our mice studies were rather low and comparable to

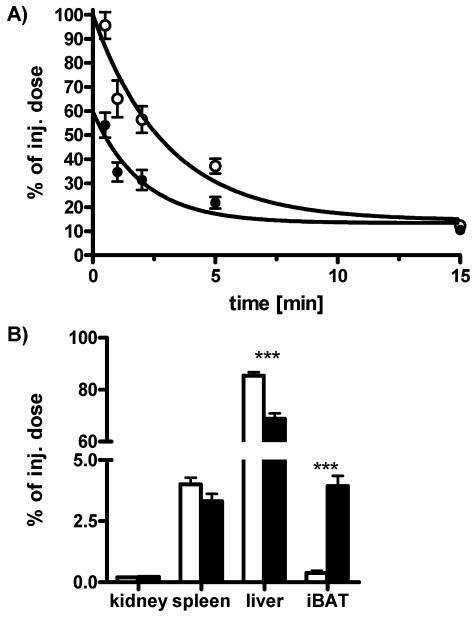

Figure 6. Quantification of nanosome uptake into BAT. Changes in the lipoprotein uptake of mice after cold exposure. (A) Blood half-life in a control group (white circles) and a cold-exposed group (black circles) FVB mice. Mean values ± sem with $n = 6$. (B) Organ distribution 15 min after i.v. injection in control (white bars) and cold-exposed (black bars) FVB mice. Mean values ± sem with $n \geq 4$ (*$p < 0.05$; **$p < 0.01$; ***$p < 0.001$).

earlier animal studies so that no radiotoxicity and no acute or chronic iron intoxication had to be expected. Furthermore, the relatively low cytotoxicity of this kind of SPIOs *in vivo* is well-described.[40] In line with this, injected ^{59}Fe-labeled nanoparticles, in a concentration which would be suitable for magnetic resonance imaging, did not induce apoptosis or alter cellular integrity in liver and kidney of mice (see Supporting Information).

Tracing Physiological Pathways. Bartelt *et al.* could recently show that lipoprotein pathways in mice can be changed by overnight cold exposition.[30] Keeping mice at low temperature (4 °C), the brown adipose tissue (BAT) is activated and changes its metabolism to the burning of lipids in order to generate heat. We used ^{59}Fe-SPIOs to quantify the uptake of triglyceride-rich lipoproteins (TRL) in brown adipose tissue upon cold exposure in more detail. After tail vein injection of recombinant TRL (similar to nanosomes) labeled with ^{59}Fe-SPIOs into cold-exposed mice, we found half of them cleared from the bloodstream within a minute compared to 3 min in the control group (Figure 6A). After 15 min, the mice were sacrificed and the organs were measured (Figure 6B). In accordance to the findings of Bartelt *et al.*, the amount of lipoproteins found in the liver was significantly decreased while significantly more ^{59}Fe was found in the BAT.[30]

CONCLUSION

In summary, we established a simple, fast, and efficient method of radiolabeling that is generally applicable for monodisperse iron oxide cores derived by high-temperature synthesis. This method does not need special equipment and can be performed "quasi on demand" in all laboratories that can work with radioisotopes. Importantly, it can be downscaled to yield high specific activities within the tolerated doses. It was demonstrated that the ^{59}Fe label is stable and can be used *in vivo*, while ^{14}C-oleic acid coating is not applicable for this purpose. These ^{59}Fe-labeled particles will make it possible to quantify MRI signals, a task frequently tried, but rarely achieved. They will also help to trace the biodistribution, clearance, and specific targeting of functionalized SPIOs in a more precise manner as hitherto possible.

MATERIAL AND METHODS

Synthesis of Iron Oxide Nanoparticles. The superparamagnetic iron oxide nanoparticles (SPIOs) were synthesized according to reported procedures (4 nm,[41,42] 6 nm,[10] 10 nm,[10] and 12 nm[43]).

Radioactive Labeling. Aliquots of a commercial ^{59}Fe-ferric chloride solution (Perkin-Elmer, Rodgau, Germany; 50−100 μCi/2−10 μg Fe) in 0.5 M hydrochloric acid were lyophilized to remove water and traces of hydrochloric acid. Then, earlier synthesized monodisperse, oleic-acid-stabilized SPIOs in chloroform were added (c = 1−5 mg SPIOs/mL). The ratio between ^{59}Fe/^{56}Fe was calculated to range between 0.01 and 0.5%. The solution was stirred at room temperature for at least 24 h before using the SPIOs for further experiments.

Water Solubilization of the Iron Oxide Nanocrystals. Encapsulation was achieved according to ref 37, with slight modifications: 2 mL of poly(maleic anhydride-*alt*-1-octadecene) (PMAOD) solution (c = 0,01 g/mL in $CHCl_3$) were added to a solution of 2 mg nanoparticles dissolved in 2 mL of chloroform and stirred at room temperature for 1 h. The solvent was then evaporated by a constant stream of N_2, and 2 mL of 20% TBE buffer was added. The solution was sonicated three times for 10 min, allowing the solution to cool between. Afterward, the solution was heated at 60 °C for 10 min. Formed aggregates were removed by centrifugation at 2400*g* (three times for 15 min), and excess polymer was removed by ultracentrifugation (1 h, 50 000*g*, 4 °C). Finally, the solution was filtered sequentially through a 0.45, 0.2, and 0.1 μm Millipore filter. The quality of the particles was confirmed by size-exclusion chromatography (SEC) and transmission electron microscopy (TEM).

Size-Exclusion Chromatography (SEC). SEC was performed using a Superose-6 10/300 GL column (Amersham Bioscience, Munich, Germany) at a flow rate of 0.5 mL/min. For iron detection, 200 μL of each fraction was treated with 50 μL of 5 M hydrochloric acid at 70 °C for 30 min.[44] Afterward, 150 μL of a 2 M acetate buffer (pH = 4.8) containing 10% ascorbic acid was added to 50 μL of each fraction, followed by 100 μL of a solution of 50 mg of bathophenanthroline in 50 mL of water. After 15 min, the absorption was measured at 540 nm.

Synthesis of ^{14}C-Oleic-Acid-Coated SPIOs. The SPIOs (core size 3 nm) were synthesized according to a reported procedure.[41] Briefly, 0.2 mmol iron(III)acetylacetonate (Strem, Kehl, Germany, 99%), 1 mmol 1,2-hexadecanediol (Aldrich, Munich, Germany 90%), 0.6 mmol [1-^{14}C]-oleic acid (Perkin-Elmer, Rodgau, Germany, >97%), 0.6 mmol oleylamine (Aldrich, 70%), and 3 mL of benzyl ether (Aldrich, 99%) were mixed and heated to 80 °C for

1 h under nitrogen atmosphere. Then the mixture was heated to 200 °C for 30 min, and finally, the solution was stirred under reflux at 270 °C for another 30 min under nitrogen. The reaction mixture was cooled to room temperature, and the SPIOs were precipitated by the addition of 12 mL of ethanol (5 min, 3260*g*). Afterward, the nanoparticles were redispersed in 1 mL of hexane. This purification step was repeated twice.

Replacement of ^{14}C-Oleic Acid by Oleic Acid or Polymer. In a vial, 20 μL of ^{14}C-oleic-acid-stabilized SPIOs (650.000 cpm/mL) was placed, and a certain amount of oleic acid or polymer dissolved in 100 μL chloroform was added. The solution was stirred at room temperature. To stop the reaction, the solvent was removed in a nitrogen stream. One milliliter of ethanol was added and the solution stirred for 90 min at room temperature. The solution was transferred to an Eppendorf cup and after centrifugation (6000*g*, 10 min), the radioactivity in 500 μL of the supernatant was measured.

Radioactivity Measurements. ^{59}Fe was measured using the large volume Hamburg whole body radioactivity counter.[45] ^{14}C-oleic acid and ^{3}H-triolein activity was measured by liquid scintillation counting.

***In Vivo* Studies.** All animal experiments were approved by the local committee for animal experiments (Behörde für Soziales, Familie, Gesundheit and Verbraucherschutz, BSG, Hamburg Tierversuchs-Nr. 34/10).

Comparison of Nanosomes Labeled with ^{3}H-Triolein, ^{59}Fe-SPIOs, or ^{14}C-SPIOs. Nanosomes were prepared according to the described procedures[29] in which the respective radiolabeled SPIOs or triolein were added. To remove free ^{59}Fe, the nanosomes were run over a PD-10 column. In anaesthetized (Rompun/Ketamine) wild-type FVB mice, 200 μL of a solution containing either nanosomes labeled with ^{3}H-triolein and ^{59}Fe-SPIOs or ^{14}C-oleic-acid-coated SPIOs was injected into the tail vein. Fifteen minutes after injection, the mice were perfused with PBS containing 10 units of heparin. The organs (spleen, kidney, and liver) were removed, and the radioactivity was measured.

Determination of the Blood Half-Life of ^{59}Fe. To determine the blood half-life, anaesthetized (Rompun/Ketamine) wild-type BALB/c mice were injected with 200 μL of a solution containing either polymer-coated ^{59}Fe-labeled SPIOs (core size 6 nm, 50 μg iron, $\geq$15000 Bq) or ^{59}Fe-SPIO nanosomes ($\geq$15000 Bq). Then, 20−50 μL of blood was taken from the retro-orbital venous plexus.

Quantification of Biochemical Processes. Anesthetised mice were injected ^{59}Fe-SPIO nanosomes into the tail vein. To determine the blood half-life, blood was taken from the retro-orbital venous plexus. After 15 min, blood was removed by cardiac puncture, the right atrium was opened, and the carcass was perfused through the left ventricle with PBS containing 50 U/mL heparin. Then, organs were removed and weighed, and their ^{59}Fe activity was measured.

Statistics. To assess statistical significance the two-tailed, unpaired Student's *t* test was performed. $P < 0.05$ was considered as significant.

Conflict of Interest: The authors declare no competing financial interest.

Acknowledgment. The technical assistance of Hendrik Herrmann, Carola Schneider, Andrea Japke, Julia Kemmling, and Angelika Schmidt is gratefully acknowledged. This work was supported by the Bundesministerium für Forschung und Technologie (BMBF, TOMCAT, project number 01 EZ 0824) and by grants from the Deutsche Forschungsgemeinschaft to P.N., J.H., and H.W. (SPP1313). O.T.B. received a fellowship of the Studienstiftung des Deutschen Volkes. A.B. is supported by a Postdoctoral Fellowship Award from the European Atherosclerosis Society and the BMBF ANCYLOSS project.

Supporting Information Available: Detailed quality control procedures for radiolabeling of monodisperse nanoparticles. This material is available free of charge *via* the Internet at http://pubs.acs.org.

REFERENCES AND NOTES

1. Thorek, D. L.; Chen, A. K.; Czupryna, J.; Tsourkas, A. Superparamagnetic Iron Oxide Nanoparticle Probes for Molecular Imaging. *Annu. Biomed. Eng.* **2006**, *34*, 23–38.
2. Laurent, S.; Boutry, S.; Mahieu, I.; Vander, E. L.; Muller, R. N. Iron Oxide Based MR Contrast Agents: From Chemistry to Cell Labeling. *Curr. Med. Chem.* **2009**, *16*, 4712–4727.
3. Mendonca Dias, M. H.; Lauterbur, P. C. Ferromagnetic Particles as Contrast Agents for Magnetic Resonance Imaging of Liver and Spleen. *Magn. Reson. Med.* **1986**, *3*, 328–330.
4. Liu, F.; Laurent, S.; Fattahi, H.; Vander, E. L.; Muller, R. N. Superparamagnetic Nanosystems Based on Iron Oxide Nanoparticles for Biomedical Imaging. *Nanomedicine* **2011**, *6*, 519–528.
5. Weissleder, R.; Stark, D. D.; Engelstad, B. L.; Bacon, B. R.; Compton, C. C.; White, D. L.; Jacobs, P.; Lewis, J. Superparamagnetic Iron Oxide: Pharmacokinetics and Toxicity. *AJR Am. J. Roentgenol.* **1989**, *152*, 167–173.
6. Kopp, A. F.; Laniado, M.; Dammann, F.; Stern, W.; Gronewaller, E.; Balzer, T.; Schimpfky, C.; Claussen, C. D. MR Imaging of the Liver with Resovist: Safety, Efficacy, and Pharmacodynamic Properties. *Radiology* **1997**, *204*, 749–756.
7. Kehagias, D. T.; Gouliamos, A. D.; Smyrniotis, V.; Vlahos, L. J. Diagnostic Efficacy and Safety of MRI of the Liver with Superparamagnetic Iron Oxide Particles (SH U 555 A). *J. Magn. Reson. Imaging* **2001**, *14*, 595–601.
8. Na, H. B.; Song, I. C.; Ichikawa, T. Inorganic Nanoparticles for MRI Contrast Agents. *Adv. Mater.* **2009**, *21*, 2133–2148.
9. Dave, S. R.; Gao, X. Monodisperse Magnetic Nanoparticles for Biodetection, Imaging, and Drug Delivery: A Versatile and Evolving Technology. *Wiley. Interdiscip. Rev. Nanomed. Nanobiotechnol.* **2009**, *1*, 583–609.
10. Hyeon, T.; Lee, S. S.; Park, J.; Chung, Y.; Na, H. B. Synthesis of Highly Crystalline and Monodisperse Maghemite Nanocrystallites without a Size-Selection Process. *J. Am. Chem. Soc.* **2001**, *123*, 12798–12801.
11. Nel, A.; Xia, T.; Madler, L.; Li, N. Toxic Potential of Materials at the Nanolevel. *Science* **2006**, *311*, 622–627.
12. Longmire, M.; Choyke, P. L.; Kobayashi, H. Clearance Properties of Nano-Sized Particles and Molecules as Imaging Agents: Considerations and Caveats. *Nanomedicine* **2008**, *3*, 703–717.
13. Bagwe, R. P.; Yang, C.; Hilliard, L. R.; Tan, W. Optimization of Dye-Doped Silica Nanoparticles Prepared Using a Reverse Microemulsion Method. *Langmuir* **2004**, *20*, 8336–8342.
14. Gul, M. O.; Jones, S. A.; Dailey, L. A.; Nacer, H.; Ma, Y.; Sadouki, F.; Hider, R.; Araman, A.; Forbes, B. A Poly(vinyl alcohol) Nanoparticle Platform for Kinetic Studies of Inhaled Particles. *Inhal. Toxicol.* **2009**, *21*, 631–640.
15. Cao, J.; Wang, Y.; Yu, J.; Xia, J.; Zhang, C.; Yin, D.; Hafeli, U. O. Preparation and Radiolabeling of Surface-Modified Magnetic Nanoparticles with Rhenium-188 for Magnetic Targeted Radiotherapy. *J. Magn. Magn. Mater.* **2004**, *277*, 165–174.
16. Liang, S.; Wang, Y.; Zhang, C.; Liu, X. Synthesis of Amino-Modified Magnetite Nanoparticles Coated with Hepama-1 and Radiolabeled with ^{188}Re for Bio-magnetically Targeted Radiotherapy. *J. Radioanal. Nucl. Chem.* **2006**, *269*, 3–7.
17. Torres Martin de Rosales, R.; Tavare, R.; Glaria, A.; Varma, G.; Protti, A.; SBlower, P. J. ^{99m}Tc-Bisphosphonate-Iron Oxide Nanoparticle Conjugates for Dual-Modality Biomedical Imaging. *Bioconjugate Chem.* **2011**, *22*, 455–465.
18. Jarrett, B. R.; Gustafsson, B.; Kukis, D. L.; Louie, A. Y. Synthesis of ^{64}Cu-Labeled Magnetic Nanoparticles for Multimodal Imaging. *Bioconjugate Chem.* **2008**, *19*, 1496–1504.
19. Gibson, N.; Holzwarth, U.; Abbas, K.; Simonelli, F.; Kozempel, J.; Cydzik, I.; Cotogno, G.; Bulgheroni, A.; Gilliland, D.; Ponti, J.; *et al.* Radiolabelling of Engineered Nanoparticles for *In Vitro* and *In Vivo* Tracing Applications Using Cyclotron Accelerators. *Arch. Toxicol.* **2011**, *85*, 751–773.
20. Chouly, C.; Pouliquen, D.; Lucet, I.; Jeune, J. J.; Jallet, P. Development of Superparamagnetic Nanoparticles for MRI: Effect of Particle Size, Charge and Surface Nature on Biodistribution. *J. Microencapsulation* **1996**, *13*, 245–255.
21. Pouliquen, D.; Perdrisot, R.; Ermias, A.; Akoka, S.; Jallet, P.; Le Jeune, J. J. Superparamagnetic Iron Oxide Nanoparticles as

a Liver MRI Contrast Agent: Contribution of Microencapsulation to Improved Biodistribution. *Magn. Reson. Imaging* **1989**, *7*, 619–627.
22. Pouliquen, D.; Lucet, I.; Chouly, C.; Perdrisot, R.; Le Jeune, J. J.; Jallet, P. Liver-Directed Superparamagnetic Iron Oxide: Quantitation of T2 Relaxation Effects. *Magn. Reson. Imaging* **1993**, *11*, 219–228.
23. Majumdar, S.; Zoghbi, S. S.; Gore, J. C. Pharmacokinetics of Superparamagnetic Iron-Oxide MR Contrast Agents in the Rat. *Invest. Radiol.* **1990**, *25*, 771–777.
24. Semmler-Behnke, M.; Kreyling, W. G.; Lipka, J.; Fertsch, S.; Wenk, A.; Takenaka, S.; Schmid, G.; Brandau, W. Biodistribution of 1.4- and 18-nm Gold Particles in Rats. *Small* **2008**, *4*, 2108–2111.
25. Schleh, C.; Semmler-Behnke, M.; Lipka, J.; Wenk, A.; Hirn, S.; Schaffler, M.; Schmid, G.; Simon, U.; Kreyling, W. G. Size and Surface Charge of Gold Nanoparticles Determine Absorption Across Intestinal Barriers and Accumulation in Secondary Target Organs after Oral Administration. *Nanotoxicology* **2012**, *6*, 36–46.
26. Ali, Z.; Abbasi, A. Z.; Zhang, F.; Arosio, P.; Lascialfari, A.; Casula, M. F.; Wenk, A.; Kreyling, W.; Plapper, R.; Seidel, M.; *et al.* Multifunctional Nanoparticles for Dual Imaging. *Anal. Chem.* **2011**, *83*, 2877–2882.
27. Lipka, J.; Semmler-Behnke, M.; Sperling, R. A.; Wenk, A.; Takenaka, S.; Schleh, C.; Kissel, T.; Parak, W. J.; Kreyling, W. G. Biodistribution of PEG-Modified Gold Nanoparticles Following Intratracheal Instillation and Intravenous Injection. *Biomaterials* **2010**, *31*, 6574–6581.
28. Marmorato, P.; Simonelli, F.; Abbas, K.; Kozempel, J.; Holzwarth, U.; Franchini, F.; Ponti, J.; Gibson, N.; Rossi, F. ^{56}Co-Labelled Radioactive Fe_3O_4 Nanoparticles for *In Vitro* Uptake Studies on Balb/3T3 and Caco-2 Cell Lines. *J. Nanopart. Res.* **2011**, *13*, 6707–6716.
29. Bruns, O. T.; Ittrich, H.; Peldschus, K.; Kaul, M. G.; Tromsdorf, U. I.; Lauterwasser, J.; Nikolic, M. S.; Mollwitz, B.; Merkel, M.; Bigall, N. C.; *et al.* Real-Time Magnetic Resonance Imaging and Quantification of Lipoprotein Metabolism *in Vivo* Using Nanocrystals. *Nat. Nanotechnol.* **2009**, *4*, 193–201.
30. Bartelt, A.; Bruns, O. T.; Reimer, R.; Hohenberg, H.; Ittrich, H.; Peldschus, K.; Kaul, M. G.; Tromsdorf, U. I.; Weller, H.; Waurisch, C.; *et al.* Brown Adipose Tissue Activity Controls Triglyceride Clearance. *Nat. Med.* **2011**, *17*, 200–205.
31. Bronstein, L. M.; Huang, X.; Retrum, J.; Schmucker, A.; Pink, M.; Stein, B. D.; Dragnea, B. Influence of Iron Oleate Complex Structure on Iron Oxide Nanoparticle Formation. *Chem. Mater.* **2007**, *19*, 3624–3632.
32. Park, J.; Joo, J.; Kwon, S. G.; Jang, Y.; Hyeon, T. Synthesis of Monodisperse Spherical Nanocrystals. *Angew. Chem., Int. Ed.* **2007**, *46*, 4630–4660.
33. Kwon, S. G.; Piao, Y.; Park, J.; Angappane, S.; Jo, Y.; Hwang, N. M.; Park, J. G.; Hyeon, T. Kinetics of Monodisperse Iron Oxide Nanocrystal Formation by "Heating-Up" Process. *J. Am. Chem. Soc.* **2007**, *129*, 12571–12584.
34. Egger, K. Der Heterogene Isotopenaustausch I. Der Austausch an Fe_3O_4 mit 59Fe. *Helv. Chim. Acta* **1963**, *148*, 1339–1354.
35. Li, H.; Brescia, R.; Krahne, R.; Bertoni, G.; Alcocer, M. J.; D'Andrea, C.; Scotognella, F.; Tassone, F.; Zanella, M.; De, G. M.; *et al.* Blue-UV-Emitting ZnSe(dot)/ZnS(rod) Core/Shell Nanocrystals Prepared from CdSe/CdS Nanocrystals by Sequential Cation Exchange. *ACS Nano* **2012**, *6*, 1637–1647.
36. Jain, P. K.; Amirav, L.; Aloni, S.; Alivisatos, A. P. Nanoheterostructure Cation Exchange: Anionic Framework Conservation. *J. Am. Chem. Soc.* **2010**, *132*, 9997–9999.
37. Shtykova, E. V.; Huang, X.; Gao, X.; Dyke, J. C.; Schmucker, A. L.; Dragnea, B.; Remmes, N.; Baxter, D. V.; Stein, B.; Konarev, P. V.; *et al.* Hydrophilic Monodisperse Magnetic Nanoparticles Protected by an Amphiphilic Alternating Copolymer. *J. Phys. Chem. C.* **2008**, *112*, 16809–16817.
38. Pellegrino, T.; Manna, L.; Kudera, S.; Liedl, T.; Koktysh, D.; Rogach, A. L.; Keller, S.; Rädler, J.; Natile, G.; Parak, W. J. Hydrophobic Nanocrystals Coated with an Amphiphilic Polymer Shell: A General Route to Water Soluble Nanocrystals. *Nano Lett.* **2004**, *4*, 703–707.
39. Heeren, J.; Bruns, O. Nanocrystals, a New Tool To Study Lipoprotein Metabolism and Atherosclerosis. *Curr. Pharm. Biotechnol.* **2012**, *13*, 365–372.
40. Yu, W. W.; Chang, E.; Falkner, J. C.; Zhang, J.; Al-Somali, A. M.; Sayes, C. M.; Johns, J.; Drezek, R.; Colvin, V. L. Forming Biocompatible and Nonaggregated Nanocrystals in Water Using Amphiphilic Polymers. *J. Am. Chem. Soc.* **2007**, *129*, 2871–2879.
41. Sun, S.; Zeng, H.; Robinson, D. B.; Raoux, S.; Rice, P. M.; Wang, S. X.; Li, G. Monodisperse MFe_2O_4 (M = Fe, Co, Mn) Nanoparticles. *J. Am. Chem. Soc.* **2004**, *126*, 273–279.
42. Sun, S.; Zeng, H. Size-Controlled Synthesis of Magnetite Nanoparticles. *J. Am. Chem. Soc.* **2002**, *124*, 8204–8205.
43. Yu, W. W.; Falkner, J. C.; Yavuz, C. T.; Colvin, V. L. Synthesis of Monodisperse Iron Oxide Nanocrystals by Thermal Decomposition of Iron Carboxylate Salts. *Chem. Commun.* **2004**, 2306–2307.
44. Huberman, A.; Perez, C. Nonheme Iron Determination. *Anal. Biochem.* **2002**, *307*, 375–378.
45. Braunsfurth, J. S.; Gabbe, E. E.; Heinrich, H. C. Performance Parameters of the Hamburg 4 π Whole Body Radioactivity Detector. *Phys. Med. Biol.* **1977**, *22*, 1–17.